

# A 40 W cw Nd:YAG solar laser pumped through a heliostat: a parabolic mirror system

Q.1 J Almeida<sup>1</sup>, D Liang<sup>1</sup>, E Guillot<sup>2</sup> and Y Abdel-Hadi<sup>3</sup>

(Ed: Janet Thomas)

<sup>1</sup> CEFITEC, Departamento de Física, FCT, Universidade Nova de Lisboa, 2829-516, Campus de Caparica, Portugal

<sup>2</sup> PROMES-CNRS, 7 rue du Four Solaire, F-66120, Font Romeu, Odeillo, France

<sup>3</sup> National Research Institute of Astronomy and Geophysics, 138 Helwan, 11722 Cairo, Egypt

E-mail: dl@fct.unl.pt

Received 13 August 2012, in final form 19 March 2013

Accepted for publication 22 March 2013

Published

Online at [stacks.iop.org/LP/23/000000](http://stacks.iop.org/LP/23/000000)

Ascii/Word/LP/  
lp469337/PAP  
Printed 23/4/2013  
Spelling US  
Issue no  
Total pages  
First page  
Last page  
File name  
Date req  
Artnum  
Cover date

## Abstract

Solar-pumped solid-state lasers are promising for renewable extreme-temperature material processing. Here, we report a significant improvement in solar laser collection efficiency by pumping the most widely used Nd:YAG single-crystal rod through a heliostat–parabolic mirror system. A conical-shaped fused silica light guide with 3D-CPC output end is used to both transmit and compress the concentrated solar radiation from the focal zone of a 2 m diameter parabolic mirror to a 5 mm diameter Nd:YAG rod within a conical pump cavity, which enables multi-pass pumping through the laser rod. 40 W cw laser power is measured, corresponding to  $13.9 \text{ W m}^{-2}$  record-high collection efficiency for the solar laser pumped through a heliostat–parabolic mirror system. 2.9% slope efficiency is fitted, corresponding to 132% enhancement over that of our previous pumping scheme. 209% reduction in threshold pump power is also registered.

Q.2 (Some figures may appear in colour only in the online journal)

## 1. Introduction

Q.3 Solar-pumped lasers have gained ever-increasing importance in recent years [1]. Compared to electrically powered lasers, solar lasers are much simpler and more reliable due to the complete elimination of electrical power generation and conditioning equipment. This technology has great potential for many applications, e.g. high-temperature material processing, free space laser communications, space to Earth power transmission, and so on.

The renewable magnesium–hydrogen cycle is also a very interesting topic for solar laser research [2]. Large amounts of heat and hydrogen ( $\text{H}_2$ ) are given off from the reaction of magnesium (Mg) with water. Magnesium has great potential as an energy source because it has an energy storage density about ten times higher than that of hydrogen. It can be easily stored and transported in the

form of ‘pellets’ and when necessary reacts with water to produce both hydrogen and thermal energy for fuel cell vehicle applications. However, 4000 K is necessary for MgO reduction [2]. Since there is no practical way of reaching this temperature by directly focusing sunlight onto MgO with conventional optics, solar-powered lasers with excellent beam quality become essential, because they can reach more than 4000 K in their focal zones. Besides, other energy cycles [3] and renewable nano-material production can also benefit from using solar-pumped lasers.

The first solar-pumped laser was reported by Young in 1966 [4]. Since then, researchers have exploited parabolic mirrors and Fresnel lenses to attain enough concentrated solar radiation at the focal point, and several pumping schemes have been proposed to enhance solar laser output performance [5–12]. The progress with Fresnel lenses and chromium co-doped Cr:Nd:YAG ceramic laser medium [9]

has revitalized solar laser research, revealing a promising future for renewable recovery of Mg from MgO.  $19.3 \text{ W m}^{-2}$  collection efficiency was reported by us in 2011 [10] by utilizing an economical Fresnel lens and the most widely used Nd:YAG single-crystal rod. The most recent Nd:YAG solar laser pumped through a large Fresnel lens and a liquid light-guide lens produced  $30.0 \text{ W m}^{-2}$  collection efficiency in 2012 [12], despite its relatively low laser beam brightness figure of merit  $B$  of  $6.6 \times 10^{-3} \text{ W}$ . Laser beam brightness is defined as the laser power divided by the product of the beam spot area and its solid angle divergence. This product is proportional to the square of the beam quality factor  $M^2$ . The brightness figure of merit  $B$  is then defined [8] as the ratio between the laser power and the product of  $M^2$  factors.

The bottle-neck limitations of present day solar lasers are their relatively low collection efficiencies and low laser beam brightnesses. The use of parabolic mirrors for solar laser research has been, in our opinion, neglected in recent years, due to the increased interest in Fresnel lenses [9, 10, 12]. We have, however, insisted on enhancing the solar laser collection efficiency with the use of parabolic mirrors. The record collection efficiency of  $6.7 \text{ W m}^{-2}$  at the Weizmann Institute of Science [8] was improved by us to  $9.6 \text{ W m}^{-2}$  in 2011 at the PROMES-CNRS, in Odeillo, France. By side pumping a 4 mm diameter Nd:YAG single-crystal rod through a single light-guide/modified 2D-CPC cavity, a record-high brightness figure of merit of  $2.9 \times 10^{-1} \text{ W}$  was registered [11]. If we consider the practical reflectivity of only less than 80% for both the heliostat and the parabolic mirror at PROMES-CNRS, and also the convenience of having a fixed focal spot for a stationary parabolic mirror, our solar laser pumped through a heliostat–parabolic mirror configuration offers a lot of practical advantages, which become more evident when very high solar laser power and excellent beam quality are needed. In contrast, a solar laser pumped through a Fresnel lens usually moves together with the whole tracking structure, and an optical fiber thus becomes essential for the transportation of laser power from the laser head to the Mg reduction vacuum chamber. Apart from a lot of practical inconvenience, fiber-optic transmission loss will inevitably be introduced, which will negatively influence the final collection efficiency of the whole laser system. A tracking heliostat–stationary parabolic mirror combination, such as the 1 MW solar collection and concentration facility at Odeillo, is more meaningful for pumping a super-high-power solar laser. It is therefore valuable for us to carry out solar laser research with parabolic mirrors.

Q.4

A large improvement in solar laser collection efficiency is reported here by pumping a 5 mm diameter, 25 mm length Nd:YAG rod through the heliostat–parabolic mirror system. Nd:YAG is the most widely used solid-state laser material and it has been demonstrated as the best material under solar pumping because of its superior characteristics of thermal conductivity, high quantum efficiency and mechanical strength compared to other host materials [4–12]. The concentrated solar radiation is first collected and transmitted through a conical-shaped fused silica light guide with a 3D-CPC output end, which further transmits and compresses

the near-Gaussian distribution from its input aperture onto the upper end face of the laser rod. The water-cooled conical pump cavity enables efficient side pumping through the laser rod due to multi-pass absorption of pump radiation. Optimum pumping conditions and solar laser beam parameters are found through ZEMAX© and LASCAD© numerical analysis respectively. The final test of the solar laser output performance was carried out at PROMES-CNRS in France during July 2012. By utilizing a medium size solar furnace (MSSF), 40.1 W cw laser power was measured, corresponding to a record-high collection efficiency of  $13.9 \text{ W m}^{-2}$  for a solar laser pumped through a heliostat–parabolic mirror system. A significant improvement in slope efficiency and a substantial reduction in threshold pump power are also promising features of our solar laser scheme.

## 2. Solar-pumped Nd:YAG laser system

A large plane mirror with 36 segments ( $0.5 \text{ m} \times 0.5 \text{ m}$  each) is mounted on a two-axis heliostat which tracks the Sun continuously, redirecting the incoming solar radiation towards a horizontal axis parabolic mirror with 2 m diameter [11], as shown in figure 1(a). An effective collection area of  $2.88 \text{ m}^2$  is calculated for the parabolic mirror. All the mirrors are back-surface silver coated, so only 59% of incoming solar radiation is focused to the focal zone, about 0.85 m away from the parabolic mirror. On high solar insolation days, more than 1.8 kW of solar power can be focused into a 15 mm diameter light spot, reaching a peak flux of  $16 \text{ W mm}^{-2}$  [13]. The laser head along with the fused silica light guide is mounted on an automatic X–Y–Z axis mechanical support and positioned at the focus of the parabolic mirror, as shown in figure 1(a).

The concentrated solar radiation at the focus is first collected by the circular input face of the fused silica light guide with conical shape, as illustrated in both figures 1(b) and 2. It is then transmitted to the light-guide output section with 3D-CPC profile, which further compresses the solar pump light, with near-Gaussian distribution, onto the 1064 nm HR end face of the rod, as observed in figure 2.

Fused silica is an ideal optical material for Nd:YAG laser pumping since it is transparent over the Nd:YAG absorption spectrum. Moreover, it has a low coefficient of thermal expansion and it is resistant to scratching and thermal shock [14]. For manufacture of the light guide, a 99.995% optical purity fused silica rod with 25 mm diameter and 100 mm length was supplied by Beijing Kinglass Quartz Co., Ltd. It was first ground and polished to produce the 3D-CPC form output end with  $D_2 = 25 \text{ mm}/D_3 = 20 \text{ mm}$  input/output diameters and  $L_2 = 20 \text{ mm}$  length, as shown in figure 2. Although the production of CPC optical surfaces is usually carried out by expensive single-point machining techniques, it is possible to approximate the complex surfaces of the CPC by means of a limited number of simpler shapes without severe efficiency losses [15]. This can simplify the production process of the light guide with 3D-CPC output end. The conical section of the light guide was then machined and polished to dimensions of  $D_1 = 22 \text{ mm}/D_2 = 25 \text{ mm}$  input/output diameters and  $L_1 = 50 \text{ mm}$  length. The polished

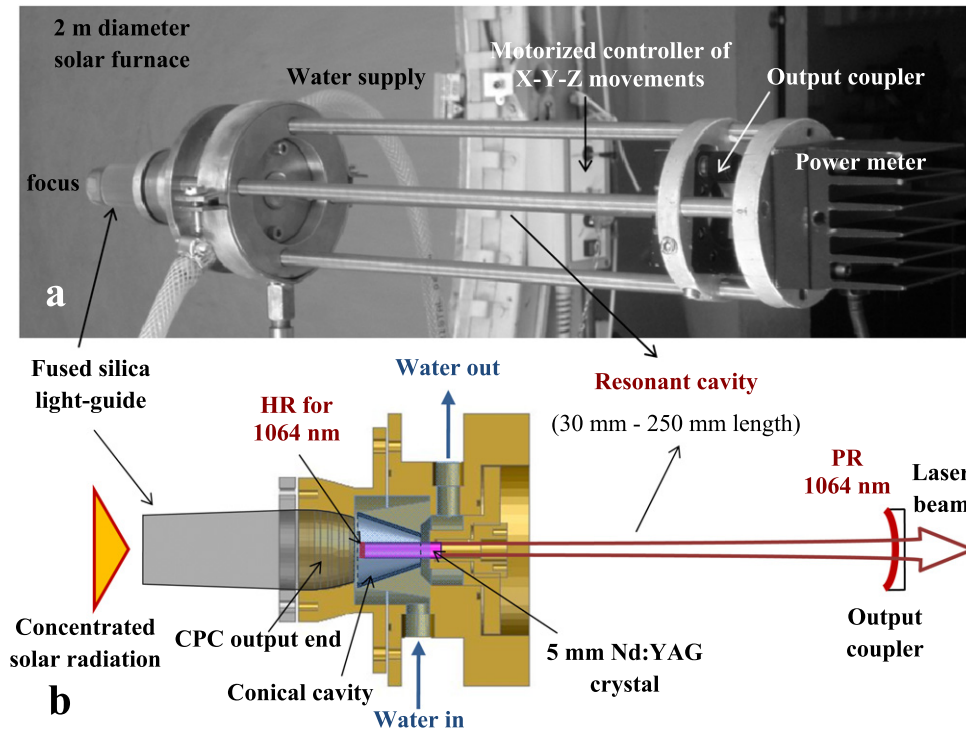


**Figure 1.** (a) The Nd:YAG laser head positioned at the focus of the PROMES-CNRS 2 m diameter parabolic mirror. (b) The mechanical structure of the Nd:YAG laser head. Both the 1064 nm HR coating and the output coupler form the laser resonant cavity.

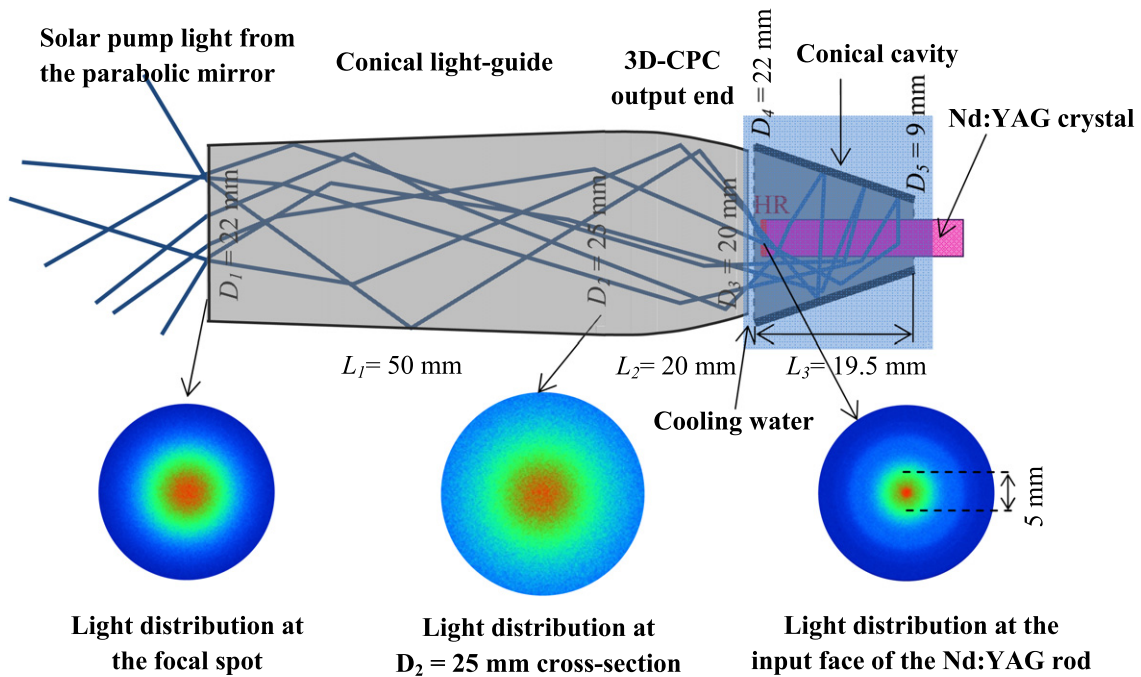


**Figure 2.** The conical-shaped fused silica light guide with 3D-CPC output end coupled to the conical pump cavity where the 5 mm diameter Nd:YAG laser rod is efficiently pumped.

light guide was finally cut away from the rest of the fused silica rod. Both the input and output ends of the light guide were finally ground and polished.

For end pumping, one part of the radiation is directly focused onto the 1064 nm HR end face of the rod by the total internal reflections from the side walls of the light guide. The

HR coating reflects the 1064 nm wavelength oscillating laser power within the resonant cavity, but allows the passage of other pumping wavelengths. Another part of the radiation not hitting the HR end face of the rod is also guided into the small conical cavity, with  $D_4 = 22 \text{ mm}/D_5 = 9 \text{ mm}$  input/output diameters and  $L_3 = 19.5 \text{ mm}$  length, which ensures efficient

side pumping to the laser rod due to multi-pass absorption of the pump radiation caused by the zigzag passage of the rays within the cavity, as shown in figure 2. The inner wall of the pumping cavity is bonded with protected silver-coated aluminum foil with 94% reflectivity. The Nd:YAG rod is actively cooled by cooling water at  $6 \text{ l min}^{-1}$  flow rate. Maximum contact between the coolant and the rod is essential for removal of the generated heat. The light-guide end face is in direct contact with the cooling water, ensuring efficient light coupling from the guide to the rod. Both fused silica material and cooling water are useful for partially preventing both UV solarization and IR heating of the laser rod. The fused silica light guide is also important in preventing the possible heating of ultra-high solar flux at the focus to the mechanical structure of the laser head.

All the design parameters are first optimized through ZEMAX© non-sequential ray-tracing software in order to obtain the maximum absorbed pump power within the Nd:YAG rod. The standard solar spectrum for one-and-a-half air mass (AM1.5) [16] is used as the reference data for the spectral irradiance ( $\text{W m}^{-2} \text{ nm}^{-1}$ ) at each wavelength. The effective pump power of the light source takes into account the 16% overlap between the absorption spectrum of the Nd:YAG medium and the solar spectrum [17]. The apparent half-angle of  $0.27^\circ$  subtended by the Sun [18] is also considered in the analysis. The absorption spectra of both fused silica and water are included in the ZEMAX© numerical data to account for absorption losses. For 1.0% Nd:YAG laser medium, 22 absorption peaks are defined in ZEMAX© numerical data [10, 11]. All the peak wavelengths and their respective absorption coefficients are added to the glass catalog for Nd:YAG material in the ZEMAX© software. Solar irradiance values for the above-mentioned 22 peak absorption wavelengths could be taken from the standard solar spectra for AM1.5 and saved as source wavelength data. In ray-tracing, the laser rod is divided into a total of 18 000 zones. The path length in each zone is found. With this value and the effective absorption coefficient of 1.0% Nd:YAG material, the power absorbed within the laser medium can be calculated by summing up the absorbed pump radiation of all zones. The absorbed pump flux data from the ZEMAX© analysis are then processed by LASCAD© software to optimize the laser resonator parameters.

The 1.0% Nd:YAG single-crystal rod was supplied by Altechna Co. Ltd. The upper end face of the rod was high reflection coated (HR) for the laser emission wavelength ( $R > 99.8\% @ 1064 \text{ nm}$ ). The lower end face was anti-reflection (AR) coated for the same wavelength ( $R < 0.2\% @ 1064 \text{ nm}$ ). The output coupler was partial reflection coated (PR). The optical laser resonator was formed by both the 1064 nm HR reflector and the PR output coupler, as demonstrated in figure 1(b), and its length could be varied from 30 to 250 mm.  $M^2$  factors could be greatly reduced in this case and higher laser beam brightness could hence be achieved. In LASCAD© software, output couplers of different reflectivity, ranging from 85% to 99%, and different radius of curvature (RoC) were tested individually to maximize the multimode laser power. According to different resonator parameters,

**Table 1.** Measurements of the solar input/Nd:YAG laser output performance for both side-pumping [11] and end-pumping configurations.

Configuration	Side pumping (2011)			End pumping (2012)		
	Reflectivity (%)	90	94	98	90	94
Slope efficiency (%)	2.2	2.0	0.9	2.9	2.8	1.7
Threshold power (W)	1100	580	402	590	334	192

various input solar power/output laser power characteristics were also numerically analyzed. An average solar pump wavelength of 660 nm and a round-trip loss of 2.1% were assumed in LASCAD© analysis.

### 3. Experimental results

The laser output power was detected by a Molectron PowerMax 500D power meter with less than 3% measurement uncertainty. Direct solar irradiance was measured simultaneously during lasing with a Kipp & Zonen CH1 pyrheliumeter on a Kipp & Zonen 2AP solar tracker. It varied between 950 and  $1020 \text{ W m}^{-2}$  during the experiments. Two sliding doors and a shutter with motorized blades were used to regulate the incoming solar power from the heliostat. To achieve the maximum laser power the shutter was totally removed.

Three  $-1 \text{ m}$  RoC output couplers with 90%, 94% and 98% reflectivity, respectively, were used to study the solar input/laser output performance. A resonator cavity length of 125 mm was adopted in this case. Figure 3 and table 1 give the comparison between the solar input/laser output performance of the present end-pumping configuration and that of our previous side-pumping configuration, carried out at PROMES-CNRS in 2011 [11].

For the solar irradiance of  $990 \text{ W m}^{-2}$  in the Odeillo area in July 2012, about 1680 W of solar power was collected by the horizontal axis medium size solar furnace in its focal zone. A maximum laser output power of 40.1 W was measured for a  $-1 \text{ m}$  RoC output coupler with 94% reflectivity, as shown in figure 3.  $13.9 \text{ W m}^{-2}$  collection efficiency was hence calculated, corresponding to an improvement of 145% over the previous results [11]. This result agrees well with the numerically predicted 39.8 W of laser power for the same resonator configuration. It is, however, limited by the practical reflectivity of both the heliostat and the parabolic mirror. If 95% reflectivity were considered for both mirrors, instead, the laser output power could be scaled up to 60 W, reaching a high collection efficiency of  $20.7 \text{ W m}^{-2}$ . A linear slope efficiency line was fitted for each output mirror reflectivity, as shown in figure 3. The highest slope efficiency of 2.9% was measured for the 90% output coupler. This value represents an enhancement of 132% over the previous Nd:YAG slope laser efficiency with side-pumping configuration. Moreover, lower pump power at the lasing threshold was measured in the focal zone for all the output mirror reflectivities. A lowest threshold pump power of 192 W was measured for the 98%

Q.5

Q.6

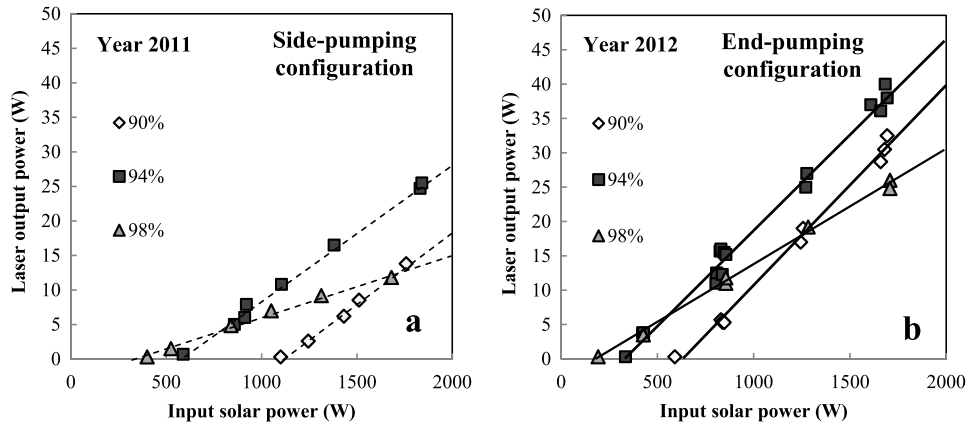


**Figure 3.** Solar input/Nd:YAG laser output performance for different output coupler reflectivities from (a) the side-pumping configuration in 2011 [11] and (b) the end-pumping configuration in 2012.

**Table 2.** Measurements of the laser performance as function of the RoC.

RoC (m)	Resonant cavity length (mm)			
	125		250	
	Laser power (W)	Figure of merit $B$ (W)	Laser power (W)	Figure of merit $B$ (W)
-0.5	36.5	$4.0 \times 10^{-2}$	—	—
-0.8	39.3	$7.4 \times 10^{-2}$	—	—
-1	40.1	$9.0 \times 10^{-2}$	33.0	$1.3 \times 10^{-1}$
-2	31.0	$1.4 \times 10^{-1}$	28.6	$1.7 \times 10^{-1}$
-5	23.1	$1.3 \times 10^{-1}$	22.0	$1.5 \times 10^{-1}$

output coupler, which is 209% less than that necessary for our previous Nd:YAG laser. The threshold power can be further reduced by increasing the output mirror reflectivity [19].

Output mirrors with optimized 94% reflectivity and RoC varying between  $-0.5$  and  $-5$  m were also used to test the solar laser performance for two different resonant cavity lengths of 125 and 250 mm. A linear fiber-optic array for measuring the one-dimensional laser beam intensity distribution was placed 5 mm and 1500 mm respectively away from the output coupler along the optical axis of the laser rod [10, 11]. A 32 mm width, 128 optical fiber linear array was used to collect and transmit laser light to a Fairchild CCD 153A 512-element linear image sensor via a neutral density attenuator. This fiber-optic device had 0.25 mm core pitch resolution, so less than 2% laser beam diameter measurement error was found. This flexible fiber-optic bundle had a length of 2 m. Outdoor solar laser beam diameter measurement was hence facilitated. The laser beam divergence  $\theta$  is found by

$$\arctan \theta = \frac{\phi_2 - \phi_1}{2L} \quad (1)$$

where  $\phi_1$  and  $\phi_2$  are the measured laser beam diameters at  $1/e^2$  width, 5 mm and 1500 mm away from the output mirror respectively, and  $L$  is the distance between these two points.  $M^2$  factors are then calculated as the ratio of the measured beam divergence  $\theta$  and that of a diffraction-limited Gaussian beam of the same wavelength, which is  $0.019^\circ$  for 1064 nm Nd:YAG laser wavelength.

Table 2 gives the measurements of both laser output power and brightness figure of merit  $B$  for the different resonator configurations.

For 125 mm resonant cavity length, high solar laser output powers of 39.3 W and 40.1 W were measured for the  $-0.8$  m RoC and  $-1$  m RoC output mirrors, respectively. A  $1.4 \times 10^{-1}$  W solar laser beam figure of merit  $B$  was calculated for the  $-2$  m RoC output mirror for the same resonant cavity length. By shifting the same RoC output mirror 250 mm away from the rod, less beam divergence was registered. A higher brightness figure of merit  $B$  of  $1.7 \times 10^{-1}$  W was hence calculated, despite the slight decrease in laser power. This value is still lower than the record-high brightness figure of merit  $B$  [11]. It is, however, 26 times higher than that of the most recent solar laser with end-pumping configuration [12].

#### 4. Conclusions

High-power and high-efficiency solar-pumped lasers have great potential for many applications. Solar lasers pumped through tracking heliostat-parabolic mirror systems can be more suitable when high-power scaling and excellent beam quality are needed. A large improvement in solar laser collection efficiency with a parabolic mirror is reported here. Due to the excellent light coupling and focusing capacity of both the fused silica light guide and the conical pump cavity, efficient end-side pumping is provided to the 5 mm Nd:YAG laser rod. 40.1 W cw laser power is measured, corresponding to  $13.9 \text{ W m}^{-2}$  collection efficiency. This value represents

an enhancement of 145% over the previous record achieved with the same solar facility. 132% improvement in slope efficiency and 209% reduction in threshold pump power are also attained, when compared to our previous scheme. A laser beam figure of merit  $B$  of  $1.7 \times 10^{-1} \text{ W}$  is registered, which is 26 times higher than that of the most recent Nd:YAG laser pumped through a Fresnel lens system. Solar-pumped lasers can benefit greatly from the advantages of heliostat–stationary parabolic mirror solar energy collection and concentration systems. Highly efficient stationary solar-pumped lasers with excellent beam quality can thus become possible.

### Acknowledgments

This research Project (no. PTDC/FIS/103599/2008) was funded by the Science and Technology Foundation of the Portuguese Ministry of Science, Technology and Higher Education (FCT-MCTES). Financial support by the Access to Research Infrastructures Activity in the 7th Framework Programme of the EU (SFERA Grant Agreement no. 228296) is gratefully acknowledged.

### Q.7 References

- [1] Graham-Rowe D 2010 *Nature Photon.* **4** 64
- [2] Yabe T et al 2006 *Appl. Phys. Lett.* **89** 261107

- [3] Steinfeld A 2005 Solar thermochemical production of hydrogen—a review *Sol. Energy* **78** 603
- [4] Young C W 1966 *Appl. Opt.* **5** 993
- [5] Arashi H, Oka Y, Sasahara N, Kaimai A and Ishigame M 1984 *Japan. J. Appl. Phys.* **23** 1051
- [6] Weksler M and Shwartz J 1988 *IEEE J. Quantum Electron.* **24** 1222
- [7] Krupkin V, Kagan J A and Yogev A 1993 *Proc. SPIE* **2016** 50
- [8] Lando M, Kagan J, Linyekin B and Dobrusin V 2003 *Opt. Commun.* **222** 371
- [9] Yabe T et al 2007 *Appl. Phys. Lett.* **90** 261120
- [10] Liang D and Almeida J 2011 *Opt. Express* **19** 26399
- [11] Almeida J, Liang D and Guillot E 2012 *Opt. Laser Technol.* **44** 2115
- [12] Dinh T H, Ohkubo T, Yabe T and Kuboyama H 2012 *Opt. Lett.* **37** 2670
- [13] Garg H P and Prakash J 2000 *Solar Energy: Fundamentals and Applications* (New Delhi: Tata McGraw-Hill)
- [14] Bernardes P H and Liang D 2006 *Appl. Opt.* **45** 3811
- [15] Jafrancesco D, Sani E, Fontani D, Mercatelli L, Sansoni P, Giannini A and Francini F 2011 *Int. J. Photoenergy* **2012** 863654
- [16] 1998 *ASTM Standard G159*
- [17] Bin Z, Zhao C, He J and Yang S 2007 *Acta Opt. Sin.* **27** 1
- [18] Abdel-Hadi Y 2005 *Development of Optical Concentrator Systems for Directly Solar Pumped Laser Systems* Mensch-und-Buch-Verlag
- [19] Koechner W 1996 *Solid State Laser Engineering* (Berlin: Springer)

Q.8

## Queries for IOP paper 469337

*Journal:* LP  
*Author:* J Almeida *et al*  
*Short title:* A 40 W cw Nd:YAG solar laser pumped  
through a heliostat: a parabolic mirror  
system

---

### Page 1

#### [Query 1:](#)

Author: Please check the author names and affiliations carefully.

---

### Page 1

#### [Query 2:](#)

Author: Please be aware that the colour figures in this article will only appear in colour in the Web version. If you require colour in the printed journal and have not previously arranged it, please contact the Production Editor now.

---

### Page 1

#### [Query 3:](#)

Author: In several places I have standardized the English somewhat. Please check that I have not inadvertently altered the meaning.

---

### Page 2

#### [Query 4:](#)

Author: Please check 'meaningful' here. Do you mean 'appropriate' or 'suitable'?

---

### Page 4

#### [Query 5:](#)

Author: Please check 'protected' here. Do you mean 'protective'?

---

### Page 4

#### [Query 6:](#)

Author: Please check the edit made in the sentence 'The standard solar spectrum ...', and correct if necessary.

---

### Page 6

#### [Query 7:](#)

Author: Please check the details for any journal references that do not have a blue link as they may contain some incorrect information. Pale purple links are used for references to arXiv e-prints.

---

### Page 6

#### [Query 8:](#)

Author: [18]: Please provide place of publication.